Published in final edited form as:
Traffic. 2012 August ; 13(8): 1072–1082. doi:10.1111/j.1600-0854.2012.01368.x.

Myosin Ia is required for CFTR brush border membrane trafficking and ion transport in the mouse small intestine

Dmitri V. Kravtsov[1], **Christina Caputo**[2], **Anne Collaco**[1], **Nadia Hoekstra**[1], **Marie E. Egan**[2,3], **Mark S. Mooseker**[4,5,6], and **Nadia A. Ameen**[1,3]

[1]Department of Pediatrics/Gastroenterology & Hepatology, Yale University, School of Medicine, New Haven, CT 06520

[2]Department of Respiratory Medicine, Yale University, School of Medicine, New Haven, CT 06520

[3]Department of Cellular and Molecular Physiology, Yale University, School of Medicine, New Haven, CT 06520

[4]Department of Molecular, Cellular and Developmental Biology, Yale University, School of Medicine, New Haven, CT 06520

[5]Department of Cell Biology, Yale University, School of Medicine, New Haven, CT 06520

[6]Department of Pathology, Yale University, School of Medicine, New Haven, CT 06520

Abstract

In enterocytes of the small intestine, endocytic trafficking of CFTR channels from the brush border membrane (BBM) to the subapical endosomes requires the minus-end motor, myosin VI (Myo6). The subapical localization of Myo6 is dependent on myosin Ia (Myo1a) the major plus-end motor associated with the BBM, suggestive of functional synergy between these two motors. In villus enterocytes of the Myo1a KO mouse small intestine, CFTR accumulated in syntaxin-3 positive subapical endosomes, redistributed to the basolateral domain and was absent from the BBM. In colon, where villi are absent and Myo1a expression is low, CFTR exhibited normal localization to the BBM in the Myo1a KO similar to WT. cAMP-stimulated CFTR anion transport in the small intestine was reduced by 58% in the KO, while anion transport in the colon was comparable to WT. Co-immunoprecipitation confirmed the association of CFTR with Myo1a. These data indicate that Myo1a is an important regulator of CFTR traffic and anion transport in the BBM of villus enterocytes and suggest that Myo1a may power apical CFTR movement into the BBM from subapical endosomes. Alternatively, it may anchor CFTR channels in the BBM of villus enterocytes as was proposed for Myo1a's role in BBM localization of sucrase-isomaltase.

Keywords

CFTR; traffic; intestine; myosin Ia; brush border; villus

Introduction

Members of the Class I myosin family of actin based motors participate in a wide range of cellular functions including membrane traffic, membrane-actin tethering, cellular motility,

Address correspondence to: Nadia Ameen, M.D, Department of Pediatrics/Gastroenterology & Hepatology, and Cellular and Molecular Physiology, Yale University School of Medicine, P.O. Box 208064, 333 Cedar St, FMP 408, New Haven, CT 06520, nadia.ameen@yale.edu Phone: 203-785-4649; Fax: 203-737-1384.

membrane channel gating and regulation of transcription (1). Myosin Ia (Myo1a), the first vertebrate myosin I to be characterized, is expressed in the intestinal epithelial cell (enterocyte).The apical brush border membrane (BBM) of the enterocyte is tethered to the underlying actin bundle within each microvillus (MV) of the BB by a spiral array of lateral bridges composed of Myo1a. Myo1a is associated with BB membrane lipid rafts and it binds to and is required for the localization of the raft associated BBM hydrolase, sucraseisomaltase (SI) (2–3). In addition to its membrane tethering function, Myo1a powers the MV-tipward movement of the BBM (3–4) to generate the formation of alkaline phosphatase (ALP)-enriched vesicles that are released from the tips of MV into the intestinal lumen and can exert antimicrobial functions (5). The enterocytes of the Myo1a knock out (KO) mouse exhibit numerous structural and compositional defects within the BB domain (3). Structural defects include detachment and extrusion of the BBM from the tips of MV, disordered MV packing, MV vesiculation and loss of the gap between the BB membrane and MV actin core. Compositional defects include loss of intra MV calmodulin (Myo1a is the major calmodulin binding protein of the BB), reduced BBM associated and basolaterally mis-localized SI, increased levels of subapical cytokeratin filaments, ectopic recruitment of Myo1c from the basolateral (BL) to BBM, and loss of two myosins from the terminal web, inter-MV membrane domain, Myo6 and Myo1e. Both of these motors have been implicated in clathrin mediated endocytosis (6–7).

In addition to its demonstrated function in tethering the BBM to the underlying actin cytoskeleton (8), Myo1a has also been proposed to play a role in the exocytic membrane traffic from the Golgi to the BBM (9). This is based on the demonstration that Myo1a is associated with isolated Golgi membrane fractions. However, evidence for a direct role for Myo1a in membrane traffic is lacking. In contrast, there is ample evidence for the involvement of Myo6, which powers movement toward the minus end of the actin filament, in endocytic membrane traffic (6). For example, in the Snell's waltzer (*sv/sv*; Myo6 mutant) mouse, endocytosis of CFTR from the enterocyte BBM is impaired, resulting in excess functional surface accumulation of CFTR (10). Two other BBM proteins that traffic between the endosome and BBM, Na+/H+ exchanger 3 (NHE3) and Na+/phosphate transporter 2b (NaPi2b), also accumulate in the BBM (11). The observed loss of Myo6 from the BB in the Myo1a KO suggests that these two motors may function synergistically in membrane traffic to and from the BBM.

Available data indicate that CFTR surface expression and anion secretion in the intestine are controlled by Myo6-dependent endocytosis, Rab11b dependent apical recycling and syntaxin 3 (Syn3) - dependent exocytic insertion of channels from subapical endosomes into the enterocyte BBM (12–14). CFTR chloride channels are the most important mediator of intestinal anion secretion from the BBM of crypt and villus enterocytes (15–16). Absence of functional CFTR on the enterocyte BBM leads to intestinal obstruction and cystic fibrosis while increased functional CFTR on the enterocyte BBM leads to excessive fluid secretion and diarrhea (10, 14, 17–19). The motor(s) that power the upward exocytic movement of CFTR to the BBM have not been identified. Given the potential of Myo1a to act synergistically with Myo6, we hypothesized that Myo1a would play a complementary exocytic role to Myo6 in regulating CFTR traffic and function in the enterocyte BBM. The current study examined BBM localization and CFTR anion transport in the intestine of Myo1a mice, and sought evidence of defective forward traffic of CFTR into the BBM of Myo1a KO enterocytes. These studies are the first to assign a specific role for Myo1a in BB localization and function of a physiologically relevant ion channel *in vivo*.

Results

Differential subcellular localization of CFTR and Myo1a in the intestine

In WT mouse small intestine, confocal microscopy of immunolabeled sections revealed apical domain staining for CFTR in all enterocytes along the villi (Fig. 1A, arrowhead) and crypt (Fig. 1A, arrow), consistent with our previous observations (20). Myo1a staining intensity in enterocytes increased from the base to the tip of the villus and its distribution overlapped with CFTR (Figure 1 B, empty arrowhead) but unlike CFTR, no apical staining for Myo1a was detected in the crypt (Fig. 1, panel B, empty arrows). Very low levels of diffuse cytoplasmic Myo1a staining were observed in crypt cells throughout the small intestine and colon (Fig. 1B, C, empty arrowhead). Previous studies have shown that unlike most MV core components (actin, villin, fimbrin) that localize to the BB in the intestine, Myo1a associates with the cytoplasm and the cell perimeter in differentiating enterocytes of the crypt (21). Its expression increases as enterocytes differentiate and at the crypt-villus transition zone, Myo1a assumes its characteristic distribution in the apical BB (21–22).

To determine whether the absence of Myo1a affects CFTR expression, immunoblot analysis of mucosal scrapings from small intestine (jejunum) was performed to compare CFTR protein in WT and Myo1a KO mice following equivalent protein loading. The typical mature fully glycosylated (~178kDa) and immature (~148kDa) CFTR bands (10, 20) were observed (Figure 1E). Total CFTR was unchanged in lysates from WT or Myo1a small intestine. Actin loading controls confirmed equal protein loading in samples (Fig. 1E). CFTR displays a proximal-distal gradient in its cellular distribution and protein expression in the intestine (20). To understand the potential relationships between Myo1a and CFTR in specific intestinal segments, Myo1a and CFTR protein expression were analyzed in WT mice (Figure 1F). When equivalent protein is loaded, CFTR displays a proximal-distal gradient of expression, with highest levels observed in the most proximal intestinal segment (duodenum) and lowest levels are observed in the most distal segment in the colon. The proximal-distal expression profile for Myo1a was quite different from CFTR. Levels of Myo1a were slightly higher in the more proximal duodenum compared to more distal segments (jejunum, ileum) of the small intestine, but levels dropped significantly in the more distal colon where it was barely detected, consistent with the localization data.

CFTR is absent from the BB in Myo1aKO intestine

The prominent co-localization of Myo1a and CFTR in the apical domain of villus enterocytes suggested that Myo1a could be a candidate motor to regulate CFTR distribution in the BB. We therefore undertook a detailed examination of CFTR localization in the BB in all major intestinal segments (including the colon) of WT and Myo1a KO with a focus on the villus compartment in segments of the small intestine, since Myo1a is not apically localized in the crypt. In all intestinal segments of WT intestine, CFTR staining was detected in the BB and was also observed in the subapical domain of enterocytes (Fig. 2A, WT, white arrowheads). In Myo1a KO tissues, little or no CFTR was detected in the BB of villus enterocytes. Instead, CFTR accumulated in vesicular structures in the subterminal web area and redistributed to the BL domain of enterocytes (Fig. 2A, Myo1a KO, empty arrows), resembling the observed changes in SI localization in the Myo1a KO (3). No change in CFTR distribution was observed in the colon of WT and Myo1a KO mice (Fig. 2A, WT or Myo1a colon, white arrowhead). These observations are consistent with the relatively low levels of Myo1a in colonic tissues compared to small intestine. Immunoblot analysis of enterocyte BB preparations isolated from Myo1a KO or control WT mice confirmed the immunofluorescence observations that CFTR was indeed absent from the BB in Myo1a KO intestine (Fig. 6B) compared to control.

Quantification of intracellular CFTR fluorescence in the BB, sub-apical and BL compartments demonstrated that CFTR lost from the Myo1aKO brush border was redistributed proportionally between the sub-apical (18%) and BL (16%) compartments (Fig. 2B). Measurements of the extent of subapical CFTR fluorescence extending into the cytoplasm from the TW indicated that in Myo1aKO villus enterocytes, the pool of subapical CFTR is increased in size and extends further into the cell compared to WT. (Fig. 2C)

CFTR accumulates in exocytic vesicles in Myo1a KO enterocytes

CFTR undergoes apical endocytic recycling and exocytosis in the intestine, and as such co-localizes with early (EEA1), apical recycling (Rab11b) and exocytic (Syn3) vesicles (12–13, 23).To characterize the compartment where CFTR accumulated beneath the terminal web in Myo1a KO villus enterocytes, double label experiments were conducted with three aforementioned markers independently using WT and Myo1a KO tissues and Caco-2_{BBE} cells (BBE). Intestinal BBE cells express the necessary cellular machinery to regulate apical endocytosis and exocytosis of endogenous CFTR and are an ideal polarized cell model for studies of CFTR trafficking in mature villus enterocytes of the small intestine (12). Knock down (KD) efficiency of Myo1a (>90%) in BBE cells was confirmed by immunoblot (supplemental Fig. 2). CFTR co-localized with all three antigens in BBE cells and tissues (Fig. 3A–C). However, CFTR accumulated more in exocytic and recycling compartments than early endosomes in the absence of Myo1a. Because the number of CFTR positive early endosomes (Fig. 3C) was significantly less than that for recycling endosomes or exocytic vesicles (Fig. 3A, B), analysis is presented in a slightly different format for EEA1 and Syn3/Rab11co-localizations with CFTR. Early endosome co-localization data are expressed as average number of EEA1-positive complexes co-localizing with CFTR, while Syn3 and Rab11 data are represented as a percentage of total intracellular CFTR co-localized to the same vesicles. Quantification of Syn3-CFTR co-labeling revealed an increase in association between CFTR and Syn3 in the subapical area of Myo1a KD enterocytes relative to the WT (Fig. 3E) while the percent of CFTR associated with Rab11 was reduced in the KD (Fig. 3D). There was a mild increase in EEA1-CFTR co-stained endosomes in Myo1a KO sections but the difference was not statistically significant (Fig. 3F). Similar to the observations in Myo1a KO tissues (Fig. 2A, empty arrow), some cells in the Myo1a KD BBE monolayers demonstrated basolateral labeling for CFTR (Fig. 3 A, B, arrows) but the redistribution was not as consistent as that observed in Myo1a KO tissues.

Myo1a-dependent localization of CFTR in the BB is specific

To determine the specificity of Myo1a for CFTR localization in the BB, CFTR was compared with two independent classes of apical membrane proteins: SLC26A6 (PAT 1), an apical chloride-bicarbonate exchanger that is expressed in the BB of villus enterocytes of the proximal small intestine (24) and functionally linked to CFTR (25–26), and ALP, the abundant non-trafficking BB enzyme (27). In all 4 major intestinal segments, no difference in BB distribution patterns of ALP was observed between WT and Myo1aKO tissues consistent with previous studies (3) (Fig. 4A). Similarly, PAT1 distribution in the BB was unaffected in KO tissues (Fig. 4B).

CFTR anion transport is impaired in Myo1a KO small intestine

To determine whether failure of CFTR to reach the BBM of villus enterocytes in Myo1a KO small intestine was of functional significance, CFTR anion transport was measured electrophysiologically in all major intestinal segments of WT and Myo1a KO mice. CFTR anion secretion was reduced in all segments (duodenum, jejunum, ileum) of the Myo1aKO small intestine compared to WT. For instance, in the duodenum there was a marked decrease in anion secretion at baseline, such that the I_{sc} in Myo1a KO tissue demonstrated only 100± 34.7 μamp/cm^2 compared to 318± 46.5 μamps/cm^2 in WT tissue. Furthermore, stimulation

with the cAMP agonist forskolin to maximally stimulate CFTR activity, only increased I_{SC} by 31.6 ± 13.7 μamps in the Myo1a KO tissue compared to 76 ± 13.6 μamps in tissue from WT animals, suggesting that there was less functional CFTR in the BBM in the Myo1a KO animals (Fig. 5). In the colon, where Myo1a expression is relatively low, CFTR anion transport in the Myo1a KO was comparable to WT as both baseline and CFTR stimulated currents were equivalent in both genotypes. The lack of detectable alterations in CFTR anion transport in the Myo1a KO colon is consistent with the WT-like normal localization patterns observed in the Myo1a KO.

CFTR forms complexes with Myo1a and silencing of Myo1a prevents apical expression of CFTR in BBE cells

To verify our observations that defective CFTR localization in Myo1a KO enterocytes resulted from the absence of Myo1a, it was necessary to confirm that CFTR and Myo1a are associated in a complex. Co-immunoprecipitation experiments were performed using BBE cell lysates as before (12). Immunoblot analysis of CFTR immunoprecipitates indicated that Myo1a and CFTR form a complex in intestinal BBE cells (Fig. 6C).

To extend this characterization for further molecular studies to dissect the role of Myo1a in BBM traffic, CFTR surface expression was examined in BBE cells following lentiviral-induced shRNA knock down (KD) of Myo1a expression. Immunoblot analysis of Myo1a confirmed significant reduction (>80%) in the level of Myo1a protein expression in KD cells (Fig. 6A, Total Myo1a). Surface and total levels of CFTR were analyzed following cell surface biotinylation and immunoblot analysis. In KD cells no surface CFTR pool was detected while total CFTR expression remained at WT level (Fig. 6A, Surface CFTR and Total CFTR accordingly). These results indicate that the BBE cell model replicates the phenotypic defect in apical delivery of CFTR observed in Myo1a KO mouse intestine.

Discussion

The current study examined the cellular and subcellular distribution of CFTR along the length of Myo1a KO mouse intestine and sought evidence for defects in CFTR BB localization and anion transport function. In contrast to its distribution in WT enterocytes, CFTR was absent from the BB and redistributed to the BL domain of mature villus enterocytes in the Myo1a KO small intestine. Consistent with lack of apical Myo1a in the crypt, CFTR distribution was unchanged in WT and Myo1a KO colon. Electrophysiological studies of Myo1a KO and WT intestinal tissues indicated that CFTR anion secretion was reduced by ~60% in Myo1a KO small intestine, consistent with absence of CFTR in the villus enterocyte BBM, while CFTR anion transport was unaffected in WT and Myo1a KO colon. Studies in BBE cells demonstrated that CFTR and Myo1a form complexes under normal conditions. With the possible exception of the role of Myo1a in localization of SI, which has been reported to be a chloride channel (28), the requirement for Myo1a in regulating BBM localization, trafficking and function of BBM ion channels or transporters has not been reported.

Membrane traffic regulates a number of epithelial transporters including CFTR. The role of unconventional myosin family members in transporter trafficking and the specific steps of myosin involvement in the cellular trafficking itineraries of epithelial transporters in polarized epithelia are poorly understood. The availability of Myo1a KO mice and well-characterized anti-CFTR antibodies that detect lower levels of endogenous CFTR in mature villus enterocytes in native intestine allowed us to directly examine the role of Myo1a in BBM localization in this cellular compartment. It also provided an opportunity to compare and contrast the major plus-end motor Myo1a in the current study with our previous observations defining the role of the major minus-end BB motor, Myo6 on CFTR

localization, trafficking and transport function in the enterocyte BBM under physiological conditions *in vivo*.

Myo1a regulates BBM delivery and CFTR anion transport in villus enterocytes

The finding in this study that CFTR fails to reach the BBM, accumulates in the terminal web region and redistributes to the BL domain of villus enterocytes in all major segments of the Myo1a KO small intestine support a dependence on Myo1a for proper CFTR localization in the villus BBM. Immunoblot analysis of equivalent protein loads of mucosal lysates from WT and Myo1a KO small intestine confirmed that total CFTR protein expression was unchanged. Quantification of changes in the intracellular CFTR distribution and extension of subapical CFTR staining into the cell demonstrated that in the Myo1a KO enterocytes CFTR lost from the BB was shared by the sub-TW space (18% increase compared to the WT) and the BL domain (16% increase compared to WT) in virtually equal proportions. Visual impression that CFTR accumulation is observed predominantly in the sub-terminal space is probably due to the more compact size of this compartment. Thus, the BL appearance of CFTR in Myo1aKO enterocytes that is also observed for SI(3), is most likely due to mis-sorting that was not investigated in the current study.

The immunofluorescent labeling data in the small intestine were supported by immunoblot analysis of purified BBs that demonstrated a significantly reduced level of CFTR in the Myo1a KO BBM. The failure of CFTR to reach the apical MV membrane when Myo1a is absent was further confirmed by surface biotinylation experiments in polarized BBE cells following KD of Myo1a mRNA expression. Absence of CFTR from the BBM was thus confirmed independently by three different approaches: immunolocalization, immunoblot analysis of the purified BBs and surface biotinylation in the Myo1a KD BBE cell cultures.

Electrophysiological studies of CFTR anion transport in WT and Myo1aKO mice demonstrated a 2.6-fold reduction in the ΔIsc (current) in Myo1a KO small intestine while no change was observed between WT and Myo1a KO colon (Fig. 5, A). The reduction in CFTR anion secretion in the small intestine is consistent with the absence of CFTR from the villus enterocyte BB. Since Myo1a is not apically localized in the crypt and its absence does not affect CFTR localization or anion transport in the colon, the residual short circuit current detected is likely mediated by crypt CFTR, which remains unaffected in the Myo1a KO intestine. The observations in this study suggest that Myo1a KO mice may be protected against cAMP-induced diarrhea, specifically the contribution of fluid secretion that originates from villus enterocytes. The signature of CFTR distribution and anion transport in the Myo1a KO intestine presents a unique intact *in vivo* model that enables independent examination of apical traffic and CFTR-anion transport in the villus compartment of the small intestine and its contribution to disease pathogenesis. The value of this model for *in vivo* studies of CFTR cannot be overemphasized in view of emerging recognition of the importance of CFTR in villus enterocyte transport function (29).

Myo1a-dependent BB localization of CFTR is specific

The results presented here support a specific role for Myo1a in CFTR delivery to the BBM on the basis of comparison of CFTR distribution with two different classes of apical BB proteins. Indeed, the demonstration that the BBM expression of other apical membrane proteins such as ALP and PAT-1 is not perturbed in the KO indicates that the failure of CFTR to localize to the BBM is not a non-specific, secondary effect of the well-documented perturbations in BBM organization in the KO (3). These data suggest the existence of non-overlapping delivery pathways for membrane proteins that could include any of the BB associated plus end myosins including Myo1a, c, e (3), and d(30), Myo2 (31), Myo5a (32),

Myo7a (33–34) Myo7b (35), Myo9b and Myo10 (33). A particularly likely candidate is Myo5b (36) which has been shown to be mutated in Microvillus Inclusion Disease (MID).

Myo1a regulates apical localization of galectin 4 and SI, two apical proteins associated with detergent resistant lipid rafts (2–3) raising the possibility that Myo1a regulates lipid raft-associated proteins in the MV environment. Thus, as discussed below, one possibility for the observed dependence of CFTR BB localization on Myo1a is that rather than exerting motor functions to power movement of CFTR from subapical endosomes, Myo1a may act in a similar fashion to its role in regulating SI by retaining CFTR in the BBM. Lipid rafts are thought to serve as markers for apical delivery (37), and indeed CFTR associates with lipid rafts in polarized epithelial cells (38). Further studies are therefore warranted to examine the molecular details of Myo1a-CFTR interactions and the potential role that lipid rafts play in CFTR retention in the enterocyte BB.

Comparisons of Myo6 and Myo1a regulation of CFTR distribution, traffic and anion transport in the intestine

Myo6, the sole minus-end directed motor in the BB, regulates clathrin-mediated endocytosis of CFTR (10). In polarized epithelia such as the small intestine, Myo6 dependent endocytosis begins when clathrin-coated pits form on the inter-MV membrane. In this location, cargo-specific recruitment of endocytic binding partners accumulate on the inner cytoplasmic surface of the plasma membrane to link surface receptors to Myo6 (6, 39). In the intestine, Myo6 is localized to the intermicrovillar domain in the terminal web region of enterocytes, consistent with its role in apical endocytosis (32, 40). Absence of Myo6 in the *sv/sv* mouse intestine leads to prominent lifting of inter-MV membrane at the bases of MV and fusion of MV analogous to that seen in *sv/sv* inner ear hair cell where fusion of stereocilia at their bases was observed (11, 40–41). In addition to the increased BBM expression of CFTR (10), NHE3 and NaPi2b there are also numerous compositional alterations including changes in endocytic components (reduced clathrin and clathrin adaptor AP2; increased Dab2; (11, 40) Since Myo6 expression in the BB of the Myo1a KO is significantly reduced (3), we expected that CFTR distribution and function in the Myo1a KO intestine would resemble that observed in the sv/sv enterocyte. Instead the pattern of CFTR distribution and function observed in Myo1a KO intestine is completely opposite to that in *sv/sv* mice lacking Myo6 (10) in that CFTR fails to be delivered to (or retained in) the BBM of villus enterocytes and results in reduced anion secretion.

Because Myo1a is a plus-end directed motor in the enterocyte BB, the observed defect in CFTR localization in Myo1a KO suggests a forward defect in exocytosis that is further supported by the co-localization data. In Myo1aKD enterocytes, the observed expansion of subapical CFTR compartment was associated with reduction in the association with Rab11-positive vesicles and an increase in the number of Syn3-CFTR positive vesicles. These results imply a defect at the very late stages of exocytosis. Since less CFTR is inserted in to the BBM, the potential pool of CFTR that is available for recycling is reduced and thus there is a shift to the exocytic compartment. Because CFTR was previously identified in early endosomes in this region (23), quantification of CFTR/EEA1 co-localization in double-labeled villus sections was conducted and suggested a trend towards greater EEA1-positive labeled vesicles in Myo1a KO enterocytes. However, the difference that we observed was not statistically significant, suggesting that there was no increase in the endocytic trafficking of CFTR.

Is Myo1a functioning as a motor or tether for CFTR in the BBM?

MV actin cores contain tropomyosin (TM) (42) that is restricted to the rootlet portion of the core in the terminal web (43). TM-containing actin filaments inhibit the motility of class I

myosins (44), including Myo1a (45) suggesting that Myo1a may not be able to traffic exocytic vesicles through the terminal web to the BBM. However, these *in vitro* studies were performed at actin and Myo1a concentrations much lower than that *in vivo*. Thus at these higher concentrations, Myo1a may have sufficient affinity for TM-actin filaments to move vesicles up the rootlet to dock and fuse with the BBM at the base of MV. Indeed, rootlet-associated vesicles have been visualized by electron microscopy (46–47). However, unlike Myo6, which is a high duty ratio motor (48) capable of endocytic movement at densities of ~ 1 motor/vesicle, Myo1a is a low duty ratio motor (49) and thus to move vesicles multiple Myo1a motors/vesicle would be required. Alternatively, Myo1a may either directly or indirectly anchor CFTR in the BBM, as has been proposed for Myo1a dependent localization of SI (2). The observation that CFTR forms a complex with Myo1a is consistent with either hypothesis. However, if Myo1a's function is to tether CFTR, then this scenario would predict an increase in the rate of apical turnover of CFTR and its accumulation in early endocytic or recycling compartment, which was not observed in this study.

The requirement for Myo1a in CFTR BB localization and function in mature villus enterocytes suggest that proper delivery of CFTR requires different actin-based motors in the crypt and villus compartments or, in fact, may be mediated by microtubule (MT) motors (presumably dynein) since under certain fixation conditions MTs have been observed to penetrate the terminal web, terminating at the bases of MV (50). Candidate motors for apical CFTR delivery in the crypt may include myosin Vb that is implicated in secretory diarrhea observed in MID (36). But no crypt-specific myosin motor that regulates CFTR exocytosis into the BBM has been identified to date.

The current studies are the first to define an important physiological role for Myo1a in regulating BBM localization and function of CFTR chloride channels, one of the most important disease relevant transporters. The apparent villus-specific trafficking and anion transport defects identified for CFTR in the Myo1a KO intestine provides a unique opportunity to further characterize the molecular interactions of Myo1a-CFTR and examine the contribution of CFTR to important global diseases such as acute infectious diarrhea that target CFTR in the villus epithelium.

Materials and Methods

Reagents and Antibodies

The following antibodies were used in this study: AME 4991 CFTR (14), alkaline phosphatase (BYA1191) (Accurate Chemicals & Scientific Corporation, Westbury, NY), myosin1a (KB1032) (51), EEA1 (Affinity Bioreagents, Golden, Colorado), Rab11 (D4F5) (Cell Signalling Technology, Boston, MA), Syn3 (Synaptic Systems, cat. # 110032, Goettingen, Germany), CFTR mm M3A7 (Millipore, Temecula, CA), 217 (Cystic Fibrosis Foundation Therapeutics, Dr. John Riordan, University of North Carolina-Chapel Hill); β-actin (Sigma-Aldrich), rhodamine-phalloidin (Invitrogen, Eugene, OR), fluorescein isothiocyanate-conjugated anti-rabbit and anti-mouse secondary (Invitrogen). All drugs and other reagents, including forskolin and amiloride were obtained from Sigma (St. Louis, MO) and J. T. Baker (Phillipsburg, NJ) unless stated otherwise.

Animals

All studies were performed with the approval of the Institutional Animal Care and Use Committee of the Yale University School of Medicine. Adult male Myo1a KO and control strain 129 (WT) mice 12–16 weeks of age were used in this study. Mice were anesthetized using Avertin (2-2-2 Tribromoethanol) 180 mg/kg administered by intraperitoneal injection and were euthanized at the end of experiments.

Cell culture

Caco-2_{BBE} (BBE) cells were obtained from American Type Culture Collection (ATCC; Manassas, VA) and grown at 37°C in 5% CO_2-90% air atmosphere in high glucose with L-glutamine Dulbecco's Modified Eagle Medium (Gibco, Glasgow, Scotland), supplemented with 10% FBS (Gibco), 10 μg/ml apo-transferrin (Sigma), 1 mM/L sodium pyruvate (Sigma), 1% penicillin-streptomycin (Gibco), 1 μg/ml Fungizone (Gibco), and 5 μg/ml Plasmocin (Invitrogen,). BBE cells were seeded at 1×10^5 cells/cm^2 onto 100-mm cell culture dishes (Corning Incorporated, Corning, NY). At 70% confluence, cells were passed onto 25-mm Transwell filters (Costar Inc., Cambridge, MA). Confluent monolayers of BBE cells were used for Western Blot analysis, immunofluorescent labeling and surface biotinylation experiments. Experiments were performed on BBE cells after 19 days in culture in all short hairpin (shRNA)-induced silencing studies.

Myo1a silencing in BBE cells

Myo1a mRNA was targeted with shRNA delivered by a lentiviral system based on a pLKO.1-Puro vector. Cells were transduced to stably express either scrambled or four different Myo1a-targeting shRNAs. Myo1a shRNAs were designed using the AsiDesigner online tool (http://sysbio.kribb.re.kr:8080/AsiDesigner/menuDesigner.jsf) and subcloned into *Age*I and *Eco*RI restriction sites of pLKO.1-TRC vector (Addgene #10878 http://www.addgene.org), immediately downstream from the U6 promoter. Scrambled shRNA in the pLKO.1-Puro vector was obtained from Addgene (#1864). The HEK-293 t/17 (ATCC) packaging cell line was transfected with the aforementioned constructs using FuGENE 6 transfection reagent (Roche Diagnostics, Indianapolis, IN) according to Addgene's protocol. Cells were plated in 25-ml flasks at 1.5×10^5 cells/ml and transfected the following day at ~70% confluence using 1 μg of shRNA-containing vector, 0.75 μg of packaging plasmid (psPAX2, Addgene #12260), and 0.25 μg of envelope plasmid (pMD2.G, Addgene #12259). Culture medium was replaced after 15 h at 37°C. Virus-containing medium was collected 24 and 48 h after transfection and titrated for optimal multiplicity of infection (MOI). Caco-2_{BBE} cells seeded at 4×10^5/ml were transduced at 60–70% confluence with polybrene (Millipore) at 5 μg/ml final concentration. Following transduction, cells were selected with 6 μg/ml puromycin (Invitrogen). shRNA-induced silencing of protein expression was assessed by Western Blot. Maximum efficiency for Myo1a mRNA silencing was achieved with M1aR1 shRNA construct (5`-AAGAATCTTCAGCTTCGCTATGA-3`) (supplemental Fig. 2). This construct was employed in all experiments involving KD cells.

Immunofluorescence Labeling and Confocal Microscopy of Tissues and Cells

Intestinal tissues were fixed in 2% (w/v) paraformaldehyde-PBS (PFA) for 1 hour at room temperature. Following fixation, tissues were cryoprotected in 30% sucrose overnight in the cold, embedded in Tissue-Tek O.C.T medium (Miles, Laboratory, Elkhardt, IN) and frozen in liquid nitrogen-cooled isopentane. Cryostat sections (5 μm) were prepared and immunolabeled as follows: all steps were carried out in a humidified chamber at room temperature, except for overnight incubation with primary antibodies, which was carried out at 4°C. Where necessary, antigen retrieval was performed by incubating sections with a solution of 1% $NaBH_4$ for 30 min. followed by 1 min. incubation in 0.1% SDS in PBS. The sections were rehydrated in PBS, and nonspecific proteins were blocked with normal goat serum and incubated with primary antibodies overnight. The sections were incubated with appropriate secondary antibodies for 1 hour, stained with rhodamine-phalloidin diluted 1:250 in PBS for 30 min. followed by 1% Hoechst nuclear stain (Sigma) and sections were mounted in Gelvatol medium. Control sections were labeled in the absence of primary antibodies or with nonspecific IgG. Similar protocol was used for Caco-2BBE cells grown on the permeable supports, except that fixation time was reduced to 10 min. at room temperature and immunolabeling was done on the permeable supports. After

immunolabeling, filters were cut and either mounted in Gelvatol or embedded in O.C.T. medium, frozen, sectioned and mounted (for XY sections) with Gelvatol. Immunolabeled sections were stored at 4°C and examined on Zeiss LSM 510-META laser scanning confocal microscope outfitted with a Chameleon laser and electronics capable of spectrally separating fluorescence emission profiles. The 510 META-based system was equipped with four separate visible lasers, including an Argon (458, 477, 488, 514 nm), DP Solid State (561 nm), HeNe (543 nm) and HeNe at (633 nm). Image acquisition and processing was achieved using ZEN (Zeiss Efficient Navigation) software. Some images were obtained using a Nikon Eclipse E800 epifluorescent microscope equipped with a Hamamatsu Orca R2-C10600 digital camera. The acquisition parameters were standardized in relation to the highest-intensity regions to avoid oversaturation of pixel intensity.

Image Quantifications

Analysis of CFTR-EEA1 co-localization was performed on confocal images of double-labeled villus sections from WT or Myo1a KO duodenum using Image J software. Confocal images were standardized as was described previously (52), converted to 2-channel (red and green) mode by subtracting Hoechst nuclear stain channel (blue). Areas of colocalized CFTR and EEA1 labeling were highlighted in white by Image J co-localization plug-in (http://rsbweb.nih.gov/ij/plugins/colocalization.html) and counted in seven WT or Myo1aKO villi. The average number of CFTR/EEA1 co-localization complexes was calculated per apical domain of the enterocyte. Analysis of CFTR-Rab11 or CFTR-Syn3 co-localization was performed in 8–10 fields of view for each of the labeling. Total intracellular CFTR signal was measured alongside with areas of colocalized CFTR and Rab11/Syn3 labeling and CFTR co-localizing with the any of the other two antigens was expressed as a percent of total intracellular CFTR. Statistical analysis was performed using Microsoft Excel and GraphPad Prism software.

Immunoblotting

Mucosal scrapings were prepared as described previously (12). Briefly, intestinal segments were harvested from anesthetized animals. Mucosal scrapings were lysed in TGH buffer (1% Triton X-100, 25 mM Hepes, and 10% glycerol, pH 7.4) containing protease inhibitors. Tissues lysates were centrifuged at 15,000 rpm for 15 min at 4 °C. Protein concentrations were determined from supernatants, samples were eluted with 2× Laemmli sample buffer (Bio-Rad) and equivalent protein loads analyzed by Western Blot as before (10).

Isolation and preparation of brush borders

Enterocytes from mouse jejunum were isolated in NET buffer (0.13 M NaCl, 5 mM EDTA, 10 mM Tris base, 0.25 mM Pefablock (Roche Diagnostics), 0.2 mM DTT, pH 7.4) containing protease inhibitors and centrifuged at 500 *g* for 10 min. Cell pellets were resuspended in NET buffer and homogenized in a mechanical homogenizer. Following homogenization, BBs were pelleted by centrifugation at 500g for 10 min., resuspended in stabilization buffer (35 mM KCl, 2 mM $MgCl_2$, 1 mM EGTA-K, 10 mM imidazole, 0.25 mM Pefablock and 0.2 mM DTT, pH 7.1), and centrifugation cycle was repeated until pure BB preparations were obtained and verified by microscopic evidence of enriched MV profiles with few cytoplasmic contaminants. Pellets were stored at −80°C overnight and resuspended in 200 μl of stabilization *buffer*, transferred to 1.5-ml Eppendorf tubes, and centrifuged at maximum speed for 30 min. Pellets were lysed in TGH buffer containing protease inhibitors on ice, and samples were analyzed by immunoblot.

Cell surface biotinylation

Polarized monolayers of filter-grown BBE cells were rinsed with 2.5 mM DTT in PBS-CM (0.1 mM $CaCl_2$ and 1.0 mM $MgCl_2$) to remove mucus from the apical surface, and incubated with freshly prepared NHS-SS-biotin (1 mg/ml) (Thermo Scientific, Rockford, IL) for 30 min on ice. Following surface labeling, cells were lysed in TGH buffer containing protease inhibitors. Equivalent amounts of protein were incubated with Immunopure immobilized streptavidin-agarose resin (Thermo Scientific) overnight at 4°C on a rocker. The following day, surface biotinylated proteins were dissociated from streptavidin-agarose by 2× Laemmli sample buffer. Cell lysates (20 μg protein) and surface biotinylated proteins were resolved by SDS-PAGE to detect either CFTR and/or Myo1a by Western Blot analysis.

Co-immunoprecipitation

Polarized cultures of Caco2 BBE cells were lysed in cold TGH buffer with added protease inhibitors and total protein content was adjusted to 4 mg/ml in 1 ml of buffer. 30 μl of Protein A Sepharose beads coated with 1 μg of anti-CFTR M3A7 or non-immune IgGs were added to the lysate and incubated at 4C overnight with continuous rocking. The following day, beads were washed and proteins were eluted off the beads with Laemmli sample buffer at 37 C. Eluates were analyzed by immunoblotting using anti Myo1a antibodies.

Ussing Chamber electrophysiological analysis

Electrophysiological analysis were performed as previously described (53). The duodenum, jejunum, ileum and distal colon were removed, cut longitudinally, washed of any intestinal contents, and mounted in the Ussing Chamber with an aperture size of 0.04 cm^2 or 0.3 cm^2 depending on intestinal segment (Physiologic Instruments, San Diego, CA). Under open-circuit conditions, the tissue was pulsed with current (1 μA for 1 sec duration every 60 seconds). From the change in the transepithelial voltage, the resistance and equivalent short circuit current were calculated according to Ohm's Law. During all experiments solutions were continuously gassed with 95%O_2/5%CO_2 and warmed to 37°C. Data was recorded continuously using the Acquire and Analyze software program (Physiologic Instruments). Initially segments were perfused with Krebs Bicarbonate Ringer's solution (KBR) and subsequently changed to a chloride-free Ringer's solution containing 5 mM barium hydroxide as previously described (54–55). Amiloride and forskolin were added to the chloride-free Ringer's solution at final concentrations of 10^{-4} M and 10^{-5} M respectively. The $CFTR_{inh}$-172 specific inhibitor was added to the final perfusate to determine the CFTR dependent portion of the I_{sc}. Amiloride and forskolin were added to the apical bath solution and $CFTR_{inh}$-172 was added to the chamber bilaterally.

Supplementary Material

Refer to Web version on PubMed Central for supplementary material.

Acknowledgments

This study was supported by National Institutes of Health R01 DK 077065 grant to N. Ameen, a DK 34989 grant to the Digestive Diseases Research Core at Yale University and NIH DK 25387 to M. Mooseker and National Institutes of Health grant P30 DK 34989 to Yale Liver Center. The authors wish to thank Lillemor Walmark for her excellent technical assistance and members of the Ameen laboratory for proof reading the manuscript.

Abbreviations

CFTR cystic fibrosis transmembrane conductance regulator

Myo6	myosin 6
Myo1a	myosin Ia
BBM	brush border membrane
BB	brush border
KO	knock out
SI	sucrase-isomaltase
CAM	calmodulin
Myo2	myosin II
MV	microvillus
WT	wild type
PFA	paraformaldehyde
NHB_4	sodium borohydride
PBS	phosphate buffered saline
NHE3	Na+/H+ exchanger 3
NaPi2b	Na+/phosphate transporter 2b

References

1. Coluccio, LM.; Myosin, I. Myosins A Superfamily of Molecular Motors. Coluccio, LM., editor. Dordrecht: Springer; 1998. p. 95-124.
2. Tyska MJ, Mooseker MS. A role for myosin-1A in the localization of a brush border disaccharidase. J Cell Biol. 2004; 165(3):395–405. [PubMed: 15138292]
3. Tyska MJ, Mackey AT, Huang JD, Copeland NG, Jenkins NA, Mooseker MS. Myosin-1a is critical for normal brush border structure and composition. Mol Biol Cell. 2005; 16(5):2443–2457. [PubMed: 15758024]
4. McConnell RE, Tyska MJ. Myosin-1a powers the sliding of apical membrane along microvillar actin bundles. J Cell Biol. 2007; 177(4):671–681. [PubMed: 17502425]
5. McConnell RE, Higginbotham JN, Shifrin DA Jr, Tabb DL, Coffey RJ, Tyska MJ. The enterocyte microvillus is a vesicle-generating organelle. J Cell Biol. 2009; 185(7):1285–1298. [PubMed: 19564407]
6. Buss F, Spudich G, Kendrick-Jones J. Myosin VI: cellular functions and motor properties. Annu Rev Cell Dev Biol. 2004; 20:649–676. [PubMed: 15473855]
7. Krendel M, Osterweil EK, Mooseker M. Myosin 1E interacts with synaptojanin-1 and dynamin and is involved in endocytosis. FEBS Lett. 2007; 581(4):644–650. [PubMed: 17257598]
8. Nambiar R, McConnell RE, Tyska MJ. Control of cell membrane tension by myosin-I. Proc Natl Acad Sci U S A. 2009; 106(29):11972–11977. [PubMed: 19574460]
9. Fath KR, Burgess DR. Golgi-derived vesicles from developing epithelial cells bind actin filaments and possess myosin-I as a cytoplasmically oriented peripheral membrane protein. J Cell Biol. 1993; 120(1):117–127. [PubMed: 8416982]
10. Ameen N, Apodaca G. Defective CFTR apical endocytosis and enterocyte brush border in myosin VI-deficient mice. Traffic. 2007; 8(8):998–1006. [PubMed: 17555536]
11. Hegan PS, Giral H, Levi M, Mooseker MS. Myosin VI is required for maintenance of brush border structure, composition, and membrane trafficking functions in the intestinal epithelial cell. Cytoskeleton (Hoboken). 2012

12. Collaco A, Marathe J, Kohnke H, Kravstov D, Ameen N. Syntaxin 3 is necessary for cAMP- and cGMP-regulated exocytosis of CFTR: implications for enterotoxigenic diarrhea. Am J Physiol Cell Physiol. 2010; 299(6):C1450–C1460. [PubMed: 20844248]
13. Silvis MR, Bertrand CA, Ameen N, Golin-Bisello F, Butterworth MB, Frizzell RA, Bradbury NA. Rab11b regulates the apical recycling of the cystic fibrosis transmembrane conductance regulator in polarized intestinal epithelial cells. Mol Biol Cell. 2009; 20(8):2337–2350. [PubMed: 19244346]
14. Golin-Bisello F, Bradbury NA, Ameen NA. Heat Stable Enterotoxin (STa) and cGMP stimulate CFTR translocation to the surface of villus enterocytes in rat jejunum and is regulated by protein kinase G. Am J Physiol Cell Physiol. 2005; 289:C708–C716. [PubMed: 15872007]
15. O'Loughlin EV, Hunt DM, Gaskin KJ, Steil D, Bruzuszcak IM, Martin HCO, Bambach C, Smith R. X-ray microanalysis of cell elements in normal and cystic fibrosis Jejunum: evidence for chloride secretion in villi. Gastroenterology. 1996; 110(No. 2):411–418. [PubMed: 8566587]
16. Pratha VS, Hogan DL, Martensson BA, Bernard J, Zhou R, Isenberg JI. Identification of transport abnormalities in duodenal mucosa and duodenal enterocytes from patients with cystic fibrosis. Gastroenterology. 2000; 118(6):1051–1060. [PubMed: 10833480]
17. Gabriel SE, Brigman KN, Koller BV, Boucher RC, Stutts MJ. Cystic fibrosis heterozygote resistance to cholera toxin in the cystic fibrosis mouse model. Science. 1994; 266:107–109. [PubMed: 7524148]
18. Park R, Grand R. Gastrointestinal Manifestations of Cystic Fibrosis: A Review. Gastroenterology. 1981; 81(6):1143–1161. [PubMed: 7026347]
19. Field M, Semrad CE. Toxigenic diarrheas, congenital diarrheas and cystic fibrosis:disorders of intestinal ion transport. Annual Review of Physiology. 1993; 55:631–655.
20. Ameen N, Alexis J, Salas P. Cellular localization of the cystic fibrosis transmembrane conductance regulator in mouse intestinal tract. Histochem Cell Biol. 2000; 114(1):69–75. [PubMed: 10959824]
21. Heintzelman MB, Mooseker MS. Assembly of the brush border cytoskeleton: changes in the distribution of microvillar core proteins during enterocyte differentiation in adult chicken intestine. Cell Motil Cytoskeleton. 1990; 15(1):12–22. [PubMed: 2403846]
22. Skowron JF, Mooseker MS. Cloning and characterization of mouse brush border myosin-I in adult and embryonic intestine. J Exp Zool. 1999; 283(3):242–257. [PubMed: 9933937]
23. Jakab RL, Collaco AM, Ameen NA. Physiological relevance of cell-specific distribution patterns of CFTR, NKCC1, NBCe1, and NHE3 along the crypt-villus axis in the intestine. Am J Physiol Gastrointest Liver Physiol. 2011; 300(1):G82–G98. [PubMed: 21030607]
24. Wang Z, Petrovic S, Mann E, Soleimani M. Identification of an apical Cl(−)/HCO3(−) exchanger in the small intestine. Am J Physiol Gastrointest Liver Physiol. 2002; 282(3):G573–G579. [PubMed: 11842009]
25. Singh AK, Sjoblom M, Zheng W, Krabbenhoft A, Riederer B, Rausch B, Manns MP, Soleimani M, Seidler U. CFTR and its key role in in vivo resting and luminal acid-induced duodenal HCO3-secretion. Acta Physiol (Oxf). 2008; 193(4):357–365. [PubMed: 18363901]
26. Singh AK, Riederer B, Chen M, Xiao F, Krabbenhoft A, Engelhardt R, Nylander O, Soleimani M, Seidler U. The switch of intestinal Slc26 exchangers from anion absorptive to HCOFormula secretory mode is dependent on CFTR anion channel function. Am J Physiol Cell Physiol. 2010; 298(5):C1057–C1065. [PubMed: 20164375]
27. Lalles JP. Intestinal alkaline phosphatase: multiple biological roles in maintenance of intestinal homeostasis and modulation by diet. Nutr Rev. 2010; 68(6):323–332. [PubMed: 20536777]
28. Finn AL, Kuzhikandathil EV, Oxford GS, Itoh-Lindstrom Y. Sucrase-isomaltase is an adenosine 3',5'-cyclic monophosphate-dependent epithelial chloride channel. Gastroenterology. 2001; 120(1): 117–125. [PubMed: 11208720]
29. Barrett, KE.; Kelly, S. Integrative Physiology and Pathophysiology of Intestinal Electrolyte Transport. In: Johnson, LR., editor. Physiology of the Gastrointestinal Tract. Fourth Edition ed.. New York: Elsevier; 2006. p. 1931-1951.

30. Benesh AE, Nambiar R, McConnell RE, Mao S, Tabb DL, Tyska MJ. Differential localization and dynamics of class I myosins in the enterocyte microvillus. Mol Biol Cell. 2010; 21(6):970–978. [PubMed: 20089841]

31. Mooseker MS, Pollard TD, Fujiwara K. Characterization and localization of myosin in the brush border of intestinal epithelial cells. J Cell Biol. 1978; 79(2 Pt 1):444–453. [PubMed: 152766]

32. Heintzelman MB, Hasson T, Mooseker MS. Multiple unconventional myosin domains of the intestinal brush border cytoskeleton. J Cell Sci. 1994; 107(Pt 12):3535–3543. [PubMed: 7706404]

33. Bement WM, Hasson T, Wirth JA, Cheney RE, Mooseker MS. Identification and overlapping expression of multiple unconventional myosin genes in vertebrate cell types. Proc Natl Acad Sci U S A. 1994; 91(14):6549–6553. [PubMed: 8022818]

34. Wolfrum U, Liu X, Schmitt A, Udovichenko IP, Williams DS. Myosin VIIa as a common component of cilia and microvilli. Cell Motil Cytoskeleton. 1998; 40(3):261–271. [PubMed: 9678669]

35. Chen ZY, Hasson T, Zhang DS, Schwender BJ, Derfler BH, Mooseker MS, Corey DP. Myosin-VIIb, a novel unconventional myosin, is a constituent of microvilli in transporting epithelia. Genomics. 2001; 72(3):285–296. [PubMed: 11401444]

36. Muller T, Hess MW, Schiefermeier N, Pfaller K, Ebner HL, Heinz-Erian P, Ponstingl H, Partsch J, Rollinghoff B, Kohler H, Berger T, Lenhartz H, Schlenck B, Houwen RJ, Taylor CJ, et al. MYO5B mutations cause microvillus inclusion disease and disrupt epithelial cell polarity. Nat Genet. 2008; 40(10):1163–1165. [PubMed: 18724368]

37. Brown DA, London E. Functions of lipid rafts in biological membranes. Annu Rev Cell Dev Biol. 1998; 14:111–136. [PubMed: 9891780]

38. Dudez T, Borot F, Huang S, Kwak BR, Bacchetta M, Ollero M, Stanton BA, Chanson M. CFTR in a lipid raft-TNFR1 complex modulates gap junctional intercellular communication and IL-8 secretion. Biochim Biophys Acta. 2008; 1783(5):779–788. [PubMed: 18255040]

39. Spudich G, Chibalina MV, Au JS, Arden SD, Buss F, Kendrick-Jones J. Myosin VI targeting to clathrin-coated structures and dimerization is mediated by binding to Disabled-2 and PtdIns(4,5)P2. Nat Cell Biol. 2007; 9(2):176–183. [PubMed: 17187061]

40. Collaco A, Jakab R, Hegan P, Mooseker M, Ameen N. Alpha-AP-2 directs myosin VI-dependent endocytosis of cystic fibrosis transmembrane conductance regulator chloride channels in the intestine. J Biol Chem. 2010; 285(22):17177–17187. [PubMed: 20351096]

41. Self T, Sobe T, Copeland NG, Jenkins NA, Avraham KB, Steel KP. Role of myosin VI in the differentiation of cochlear hair cells. Dev Biol. 1999; 214(2):331–341. [PubMed: 10525338]

42. Mooseker MS. Brush border motility. Microvillar contraction in triton-treated brush borders isolated from intestinal epithelium. J Cell Biol. 1976; 71(2):417–433. [PubMed: 11222]

43. Bretscher A, Weber K. Tropomyosin from bovine brain contains two polypeptide chains of slightly different molecular weights. FEBS Lett. 1978; 85(1):145–148. [PubMed: 620785]

44. Tang N, Ostap EM. Motor domain-dependent localization of myo1b (myr-1). Curr Biol. 2001; 11(14):1131–1135. [PubMed: 11509238]

45. Fanning AS, Wolenski JS, Mooseker MS, Izant JG. Differential regulation of skeletal muscle myosin-II and brush border myosin-I enzymology and mechanochemistry by bacterially produced tropomyosin isoforms. Cell Motil Cytoskeleton. 1994; 29(1):29–45. [PubMed: 7820856]

46. Hirokawa N, Keller TC 3rd, Chasan R, Mooseker MS. Mechanism of brush border contractility studied by the quick-freeze, deep-etch method. J Cell Biol. 1983; 96(5):1325–1336. [PubMed: 6601660]

47. Mooseker MS, Bonder EM, Conzelman KA, Fishkind DJ, Howe CL, Keller TC 3rd. Brush border cytoskeleton and integration of cellular functions. J Cell Biol. 1984; 99(1 Pt 2):104s–112s. [PubMed: 6378918]

48. De La Cruz EM, Ostap EM, Sweeney HL. Kinetic mechanism and regulation of myosin VI. J Biol Chem. 2001; 276(34):32373–32381. [PubMed: 11423557]

49. Jontes JD, Milligan RA, Pollard TD, Ostap EM. Kinetic characterization of brush border myosin-I ATPase. Proc Natl Acad Sci U S A. 1997; 94(26):14332–14337. [PubMed: 9405612]

50. Hagen SJ, Allan CH, Trier JS. Demonstration of microtubules in the terminal web of mature absorptive cells from the small intestine of the rat. Cell Tissue Res. 1987; 248(3):709–711. [PubMed: 3607856]

51. Skowron JF, Bement WM, Mooseker MS. Human brush border myosin-I and myosin-Ic expression in human intestine and Caco-2BBe cells. Cell Motil Cytoskeleton. 1998; 41(4):308–324. [PubMed: 9858156]

52. Kirkeby S, Thomsen CE. Quantitative immunohistochemistry of fluorescence labelled probes using low-cost software. J Immunol Methods. 2005; 301(1–2):102–113. [PubMed: 15982663]

53. Grubb BR. Bioelectric measurement of CFTR function in mice. Methods Mol Med. 2002; 70:525–535. [PubMed: 11917548]

54. Weiner SACC, Bruscia E, Ferreira EC, Price JE, Krause DS, Egan ME. Rectal Potential Difference and the Functional Expression of CFTR in the Gastrointestinal Epithelia in Cystic Fibrosis Mouse Models. Pediatric Research. 2008; 63(1):73–78. [PubMed: 18043508]

55. Bruscia EM, Price JE, Cheng EC, Weiner S, Caputo C, Ferreira EC, Egan ME, Krause DS. Assessment of cystic fibrosis transmembrane conductance regulator (CFTR) activity in CFTR-null mice after bone marrow transplantation. Proc Natl Acad Sci U S A. 2006; 103(8):2965–2970. [PubMed: 16481627]

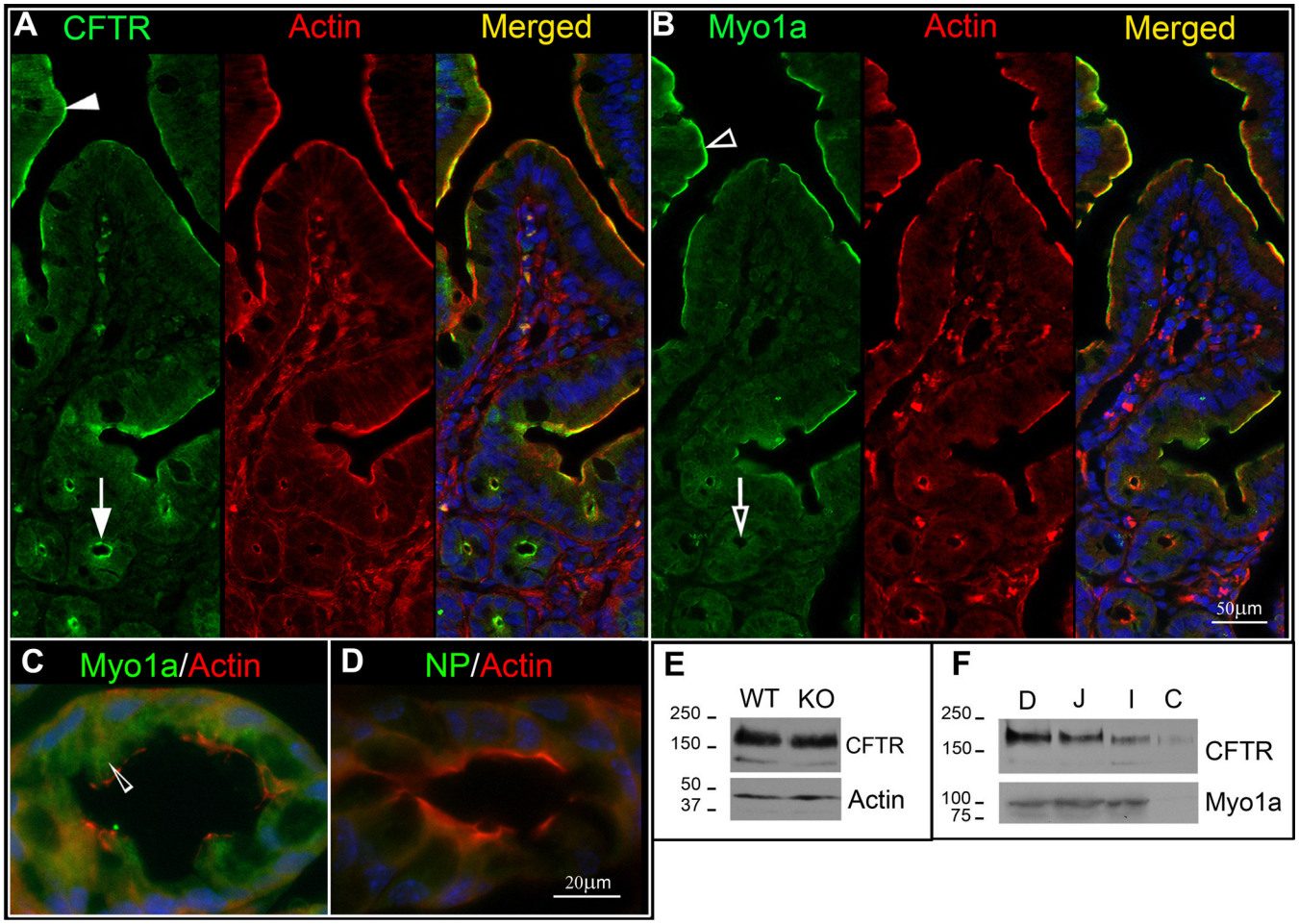

Fig.1. Distribution and expression of CFTR and Myo1a in the mouse intestine

Staining for CFTR (green), F-actin (red) and nuclei (blue) in WT mouse jejunum. A. CFTR staining in the apical domain of villus (filled arrowhead) and crypt (arrow) enterocytes. B. Staining for Myo1a (green). F-actin (red) and nuclei (blue) in WT mouse jejunum. Myo1a Staining in apical domain of enterocytes on the villi (empty arrowhead) and crypts (empty arrow) C. Double label of Myo1a (green) and F-actin (red) reveals cytoplasmic Myo1a staining (empty arrowhead) in WT mouse colon. D. Control staining in absence of Myo1a antibody. NP, non-immune primary control. E. Immunoblot analysis of equivalent protein loads (20ug) for CFTR and actin in lysates from WT129 (WT) and Myo1a KO (KO) mouse jejunum. Fully glycosylated band C (~178kDa) and immature band B (~148kDa) of mouse CFTR are identified. F. Immunoblots of equivalent protein load (20ug) analyzed for CFTR and Myo1a in major intestinal segments of WT mouse. D: duodenum, J: jejunum, I: ileum, C: colon. Molecular markers indicated in kDa.

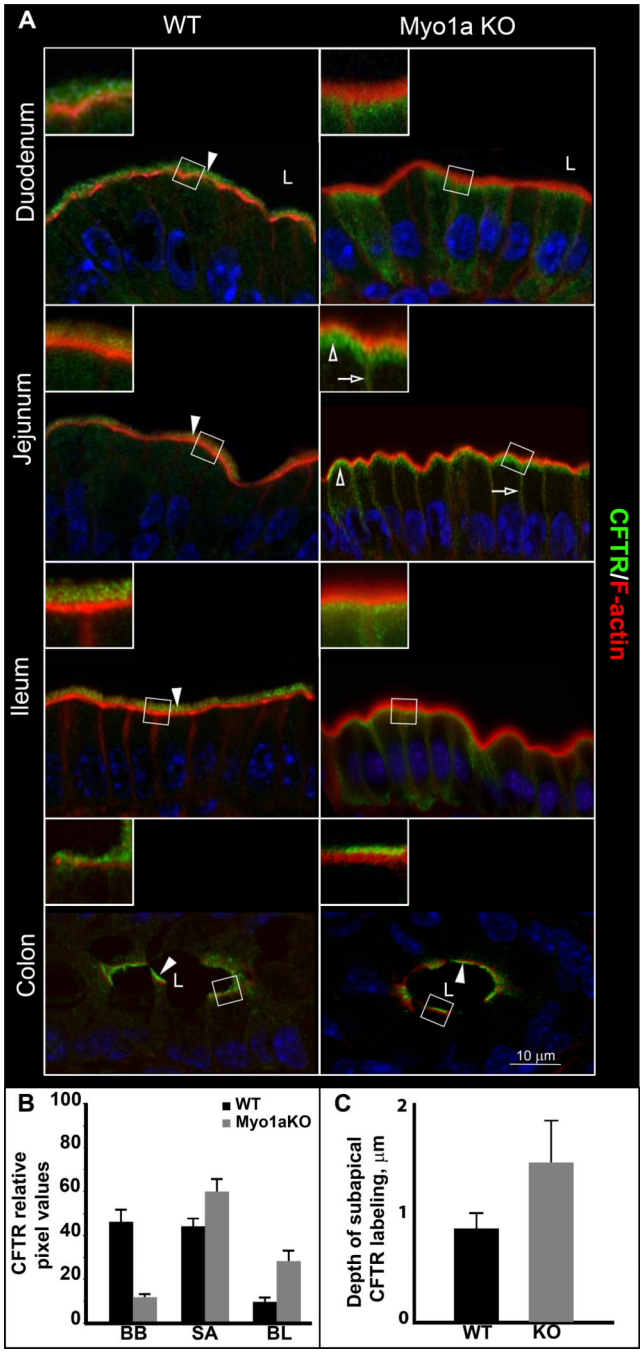

Fig.2. Distribution of CFTR and F-actin in major intestinal segments of WT129 and Myo1a KO mice

A. CFTR (green) staining is shown in relation to F-actin (red), nuclei are stained in blue. Brush border localization for CFTR is indicated with filled arrowheads throughout the WT129 intestine and in the Myo1a KO colon. Redistribution of CFTR staining in the small intestine of Myo1a KO is indicated with empty arrows (BL) and empty arrowheads (SA). L, lumen of intestine. B. Quantification analysis of changes in CFTR distribution. Data are presented as means of percent of total intracellular CFTR in BB, SA or BL compartments. WT BB, 46.2±5.9; WT SA, 44.1±3.9; WT BL, 9.7±2.3; KO BB, 11.9±1.7; KO SA, 60±6.1;

KO BL, 28.2±5.1. C. Average distance (um) of CFTR staining extending from the lumen into the subapical domain of villus enterocytes in WT and Myo1KO.

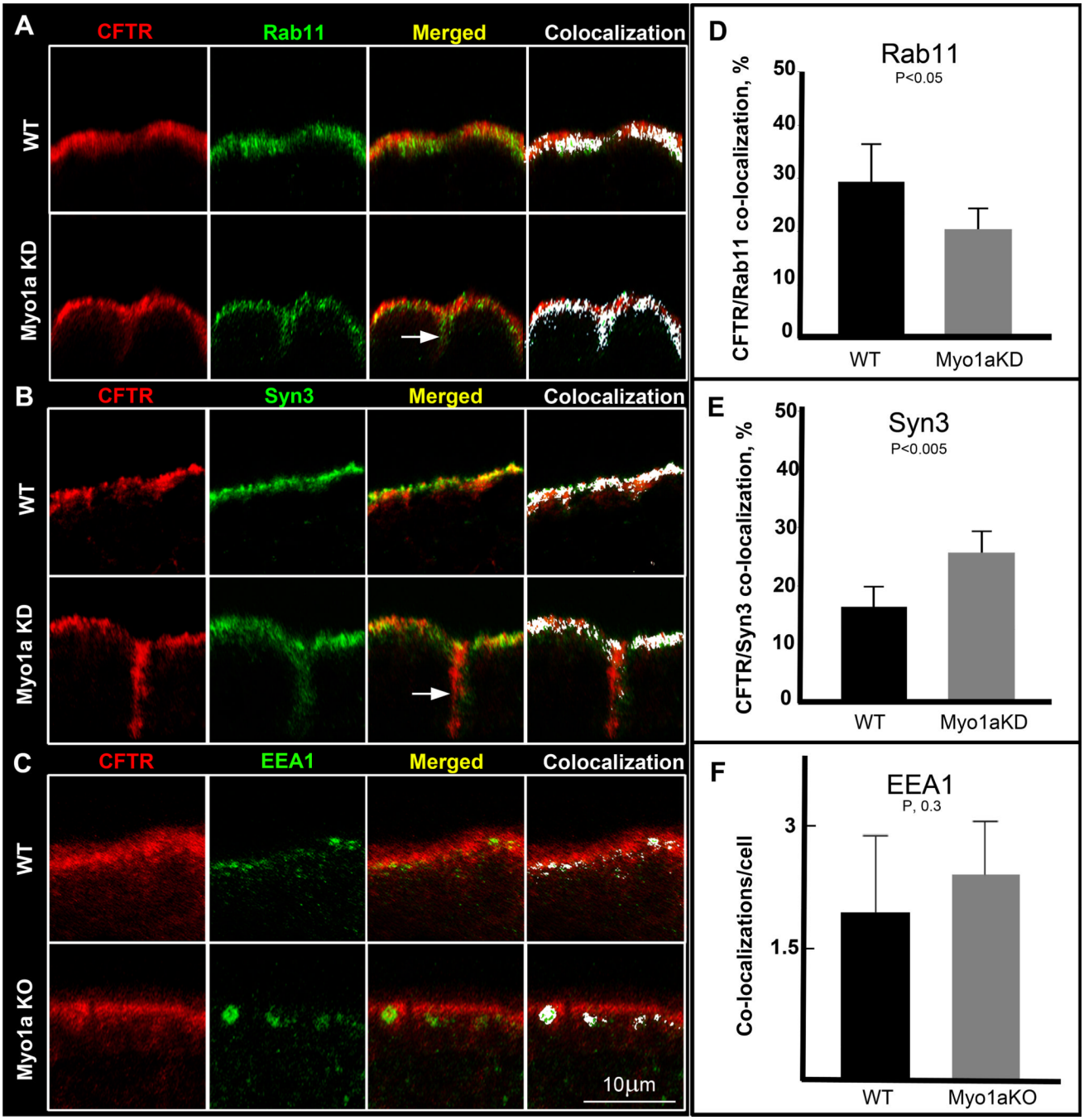

Fig.3. CFTR co-localization with endosomal markers in apical domain of WT and Myo1aKO duodenal villus entercytes

Representative confocal images of sections of polarized Caco-2_{BBE} cell monolayers double labeled for CFTR (red) and Rab11 (A) or Syn3 (B) (green), or duodenal section from WT and Myo1a KO mice double labeled for CFTR (red) and EEA1 (green) (C), with areas of antigen co-localization highlighted in white. Arrows indicate basolateral staining. D, E, F. Graphs of quantification analysis of CFTR/Rab11, CFTR/Syn3 and CFTR/EEA1 co-localization. The date are shown as means of percentage of apical CFTR co-localized with Rab11 or Syn3 or as means of apical CFTR/EEA1 complexes per enterocyte; D. Percent of total intracellular CFTR co-localizing with Rab11: WT, 29.2+−7.3; Myo1aKD, 20.3+−4.3.

E, Percent of total intracellular CFTR co-localizing with Syn3: WT, 16.4+−3.5; Myo1aKD, 25.7+−4 F, analysis yielded an average of 1.97±0.9 areas of co-localization per WT enterocyte and 2.41±0.65 per Myo1aKO enterocyte. Bar, 10um.

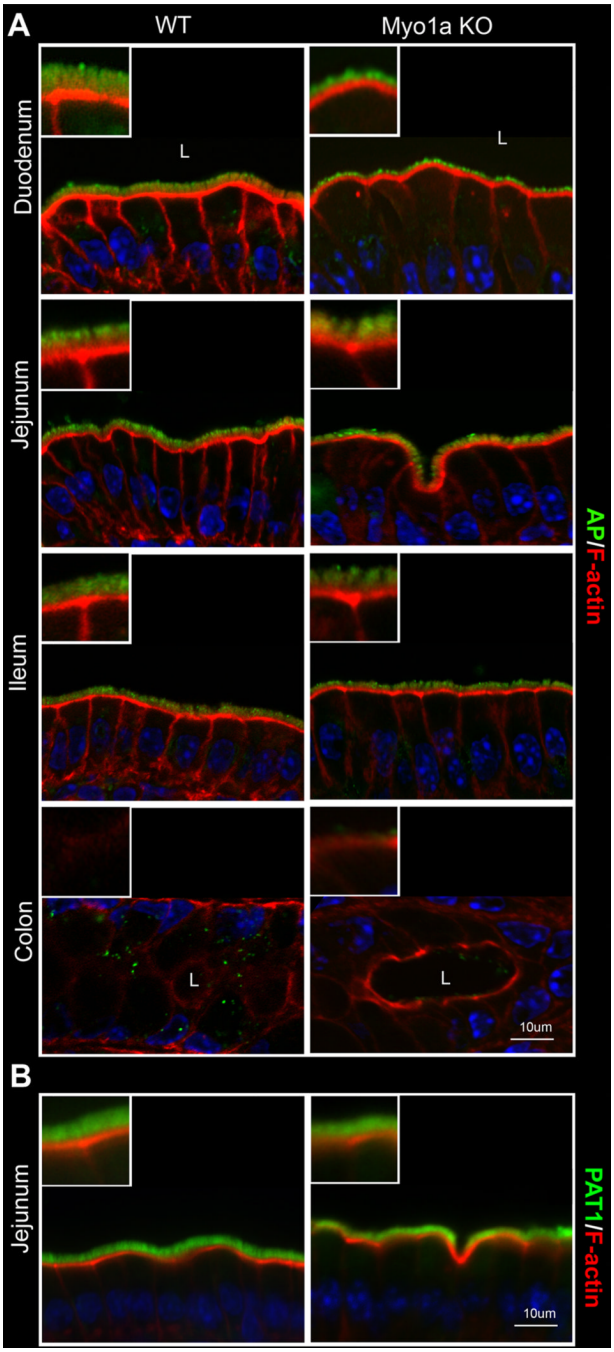

Fig.4. Distribution of alkaline phosphatase (AP) and PAT1 in major segments of WT129 and Myo1a KO intestine

A. BB alkaline phosphatase (AP) (green) and F-action (red) staining in section of WT 129 and Myo1a KO duodenum, jejunum ileum and colon B. BB PAT1 (green) and F-actin (red) staining in villus sections of WT129 and Myo1a KO jejunum. Nuclei are stained in blue; L, lumen of intestine.

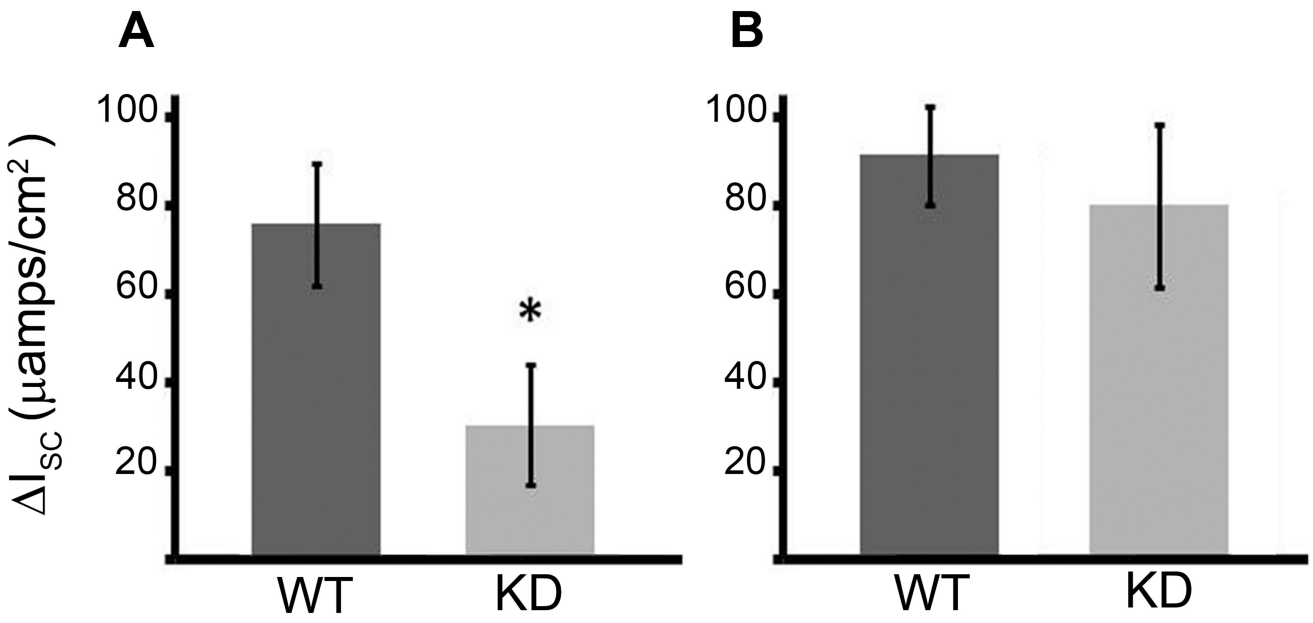

Fig.5. Ussing chamber transepithelial CFTR currents in Myo1a KO and WT129 small intestine and colon

A. Increase in Isc (μamps/cm^2) after maximal stimulation with forskolin in WT (n=3) and Myo1a KO (n= 5) duodenal tissue (* $p < 0.038$). B. Increase in Isc (μamps/cm^2) after maximal stimulation with forskolin in WT (n=4) and Myo1a KO (n=3) distal colonic tissue.

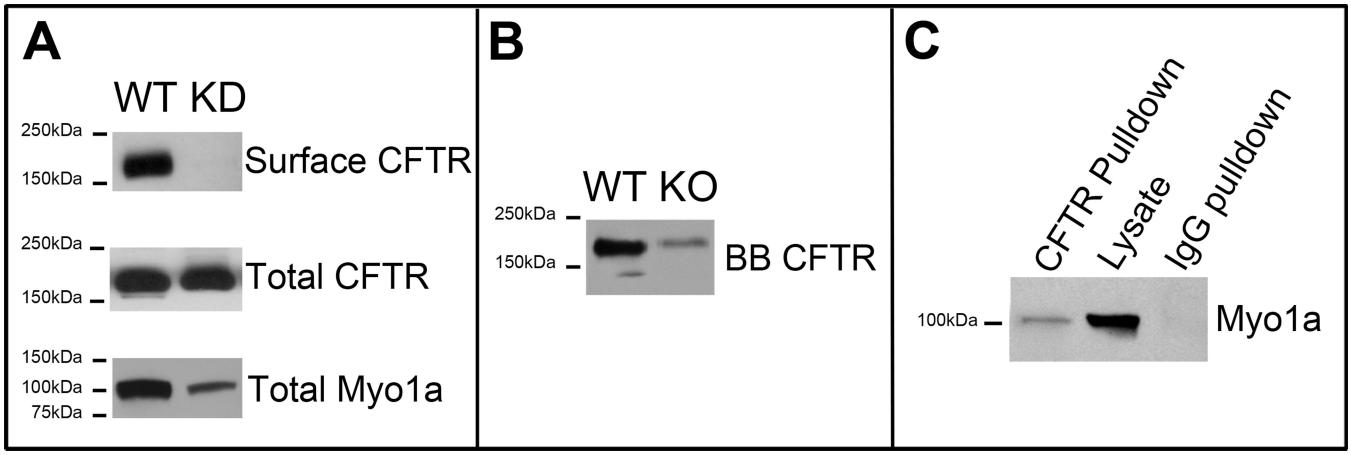

Fig.6. Efficient shRNA- induced silencing of Myo1a expression abrogates surface CFTR in polarized CaCo-2_{BB}E cells

A. Immunoblot analysis of CFTR and Myo1a in BBE cells following shRNA-induced silencing of Myo1a expression. Surface proteins were labeled at 4° C using sulpho-NHS-SS-biotin and biotinylated CFTR was recovered with streptavidin agarose. Immunoblot of total CFTR and Myo1a from the same cell lysated normalized for total protein content. B. Immunoblot detection of CFTR in purified BBs from WT129 (WT) and Myo1a KO small intestine. C. CFTR pull-downs from the Caco-2_{BBE} lysates immunoblotted for Myo1a.